

● *Original Contribution*

COMPUTER ANALYSIS AND PATTERN RECOGNITION OF DOPPLER BLOOD FLOW SPECTRA FOR DISEASE CLASSIFICATION IN THE LOWER LIMB ARTERIES

LOUIS ALLARD,^{†‡} YVES E. LANGLOIS,^{†‡} LOUIS-GILLES DURAND,[†]
GHISLAINE O. ROEDERER,[‡] MANON BEAUDOIN,[‡] GUY CLOUTIER,[†]
PAUL ROY* and PIERRE ROBILLARD*

[†]Biomedical Engineering Laboratory, Clinical Research Institute of Montreal, 110 Avenue des Pins Ouest, Montréal, Québec, Canada, H2W 1R7; [‡]Noninvasive Cardiovascular Research Laboratory, Hôtel-Dieu de Montréal Hospital, 3840 Rue St-Urbain, Montréal, Québec, Canada, H2W 1T8; *Radiology Division, Hôtel-Dieu de Montréal Hospital, 3840 Rue St-Urbain, Montréal, Québec, Canada, H2W 1T8

(Received 2 February 1990; in final form 13 September 1990)

Abstract—In the present study, a computer processing method was developed to objectively classify disease in the lower limb arteries evaluated by noninvasive ultrasonic duplex scanning. This method analyzes Doppler blood flow signals, extracts diagnostic features from Doppler spectrograms and classifies the severity of the disease into three categories of diameter reduction (0–19%, 20–49% and 50–99%). The features investigated were based on frequency features obtained at peak systole, spectral broadening indices and normalized amplitudes of the power spectrogram computed in various positive and negative frequency bands. A total of 379 arterial segments studied from the aorta to the popliteal artery were classified using a pattern recognition method based on the Bayes model. Two classification schemes using a two-node decision rule were tested. Both schemes gave similar results, the first one provided an overall accuracy of 83% ($Kappa = 0.42$) and the second an overall accuracy of 81% ($Kappa = 0.35$) when compared with conventional biplane contrast arteriography. These performances, especially for the 0 to 19% lesion category, are better than the one obtained by the technologist (accuracy = 76% and $Kappa = 0.33$), based on visual interpretation of the Doppler spectrograms. To recognize hemodynamically significant stenoses (50–99% lesions), the pattern recognition system has a sensitivity and a specificity of 50% and 99%, respectively, using classification scheme I. With classification scheme II, the sensitivity and the specificity are 50% and 98%, respectively. Visual interpretation of the Doppler spectrograms leads to a sensitivity and a specificity of 50% and 98%, respectively. These results are the first to be obtained by a pattern recognition system in classifying lower limb arterial stenoses.

Key Words: Ultrasound, Doppler techniques, Atherosclerosis, Peripheral artery disease, Spectral analysis, Frequency contour estimation, Pattern recognition.

INTRODUCTION

The ultrasonic duplex scanner, which combines real-time B-mode imaging and pulsed Doppler blood flow recording systems, has allowed important progress in the detection of arterial disease (Strandness 1985). However, assessment of lower limb arterial stenoses

using duplex scanning has been mainly performed by visual interpretation of the pulsed Doppler blood flow spectra (Langsfeld et al. 1988; Kohler et al. 1987a; Jager et al. 1985; Walton et al. 1984). The results reported by these groups for detecting greater than 50% diameter reducing lesions yielded a sensitivity varying between 77% and 87% and a specificity varying between 88% and 93%. Although accurate for detecting severe stenoses, the approach proposed by these investigators showed poor performance (percentage of correct classification varying between 35% and 76%) in classifying arterial disease in a multiclass decision level. The use of a more quantitative and objective approach to analyze the Doppler velocity waveforms

Address correspondence, reprint and software requests to: Louis Allard, Clinical Research Institute of Montreal, 110 Avenue des Pins Ouest, Montréal, Québec, Canada, H2W 1R7.

The signal processing software package (excluding the pattern recognition software) is available. It is written in C language and run on a compatible IBM-386 system having at least 1 Mbyte of extended memory. A small charge might be incurred to cover the cost of the computer diskettes and expedition.

and to classify the degree of stenosis is thus highly desirable.

The computer analysis of Doppler blood flow signals requires efficient and robust algorithms to perform arterial stenosis classification. A critical problem with Doppler blood flow digital signal processing is to estimate the minimum and maximum frequency contours of the spectrograms. This estimation constitutes a preliminary step because extraction of the discriminant features is performed only within the area delimited by the frequency contours. Using the ensemble of discriminant features selected, a pattern recognition system must then be designed to classify Doppler blood flow signals according to the percentage of stenosis. Such an approach has proved to be very accurate in the classification of disease at the carotid bifurcation (Langlois et al. 1984; Greene et al. 1982).

Different computer-based algorithms have been proposed to estimate frequency contours of Doppler spectrograms. Some of the proposed methods use frequency bandwidths estimated at levels varying from -3 to -12 dB below the mode of each spectrum (Hutchison and Karpinski 1988; Rittgers et al. 1983; Greene et al. 1982). Using cardiac Doppler signals, Cloutier et al. (1989) have demonstrated that minimum and maximum frequency contours allow extraction of spectral features with better discriminating power than those extracted from the frequency bandwidth contours. The general approach to determine minimum and maximum frequency contours is to estimate the background noise level and compute a threshold level allowing an optimal discrimination between signal and noise. Recently, Mo et al. (1988) have evaluated the performance of the following methods on a simulated carotid spectrogram: the percentile method, the D'Alessio's threshold crossing method, the modified threshold crossing method and the hybrid method. Cloutier et al. (1990) improved some of these algorithms and evaluated them on clinical cardiac Doppler signals. However, the main problem with these algorithms is the use of a threshold level whose value is not adapted to the characteristics and amplitude of the Doppler blood flow signals. Since the latter greatly vary from one patient to another and from one sample site to another, the estimation of the frequency contours is not always optimal. To take these variations into account, an iterative approach based on a modified percentile method is presented in this paper.

Another difficulty encountered in the quantitative analysis of Doppler waveforms is the extraction of features having a high discriminant value. Before the introduction of duplex scanning, features extracted from the common femoral artery were used to

evaluate stenoses of the aortoiliac segment. The spectral features used in such an approach were based on the evaluation of the pulsatility index (Johnston et al. 1983; Gosling et al. 1971) and the Laplace transform coefficients (Skidmore and Woodcock 1980a, 1980b). These features have not achieved widespread use or acceptance since they are affected by distal stenoses or constitute poor predictors of lower grade stenoses (Reddy et al. 1986; Baker et al. 1984; Evans et al. 1980; Skidmore et al. 1980c). Moreover, both features are inappropriate for detecting distal disease in the femoropopliteal segment (Baker et al. 1989; Johnston et al. 1984). The duplex scanner has the advantage of allowing acquisition of Doppler signals at various sites from the aorta down to the popliteal artery. This was demonstrated by Jager et al. (1985) who defined and used some visual criteria based on peak systolic velocity, diastolic reverse flow and spectral broadening indices to assess the severity of peripheral arterial disease. Using duplex scanning and a more quantitative approach of analysis, it is expected that more reliable and consistent results could be obtained.

The purpose of this paper is to describe a computerized method based on spectral analysis and pattern recognition of Doppler blood flow signals for objective and accurate classification of lower limb arterial stenoses. The classifier was designed to categorize arterial stenoses into three classes: 0 to 19%, 20 to 49% and 50 to 99% diameter reducing lesions. All arterial segments studied from the aorta down to the popliteal artery were classified using the same classifier. Results obtained from the evaluation of a total of 379 arterial segments are presented. The performance of the pattern recognition method was compared to the classification of disease obtained by conventional biplane contrast angiograms read independently by an experienced angiologist.

MATERIALS AND METHODS

Patient selection and data acquisition

Subjects for this study were recruited among patients referred to the Hôtel-Dieu de Montréal Hospital for arteriographic examination of the lower limb arteries. All patients scheduled for arteriography gave informed consent as required by the Ethic Committee of Hôtel-Dieu de Montréal Hospital. Only patients for which the arteriographic examination was performed within 3 months of the Doppler examination were included. Doppler studies were performed with an Ultramark 8 Duplex scanner (Advanced Technology Laboratories) modified to allow the recording of the two quadrature Doppler signals on a four-channel audio tape recorder (TASCAM 22-4) for off-line analysis. These signals correspond to the inputs of the

phase shifter whose outputs are the forward and reverse flow channels. The ECG signal was also recorded on a FM-carrier signal and used to detect the beginning of each cardiac cycle. Voice comments indicating the patient's name and the sites analyzed were recorded on the fourth channel.

The arterial segments examined in each limb were: the distal aorta, the common and external iliac arteries, the common and profunda femoral arteries, the superficial femoral artery, and the popliteal artery. A mechanically oscillating probe, operating at 5 MHz, was used for all Doppler recordings. The sample volume was placed in the centerstream of the artery where flow velocities are maximal. According to the manufacturer's specifications, the sample volume used for all recordings had a length of 1.5 mm in the direction of the axial beam, which is much smaller than the diameter of the arterial segments studied. For each segment analyzed, Doppler blood flow signals were recorded for a period of approximately 20 s. Segments were initially probed to assess the presence or absence of disease. Representative signals from all segments were recorded at midcourse of the segment if normal or at the site of most severe disease. The latter was identified by the technologist at the site of maximal flow disturbances, spectral broadening or increased Doppler frequencies. In order to standardize the recordings, the patients were asked to rest supine at least 30 min in a controlled temperature environment (21–23°C). The high-pass filter used to remove noise attributable to motion effects was set at 100 Hz. Since the duplex scanner can only determine the angle between the sound beam and the vessel axis and since arterial blood flow is not always parallel to the axis of the artery, we felt that it was essential to standardize the recordings by performing them at a constant angle between transducer and blood vessel axis (Beach *et al.* 1989; Phillips *et al.* 1989). For that reason, we maintained a standard angle as close as possible to 60 degrees between the Doppler beam and blood vessel axis for all recordings.

The Doppler signal processing was performed on a 16 MHz IBM-PC/386 compatible personal computer. During tape playback, ECG and Doppler signals were digitized with a 12-bit analog-to-digital (A/D) converter at sampling rates of 2 kHz and 20 kHz, respectively. Before digitization, Doppler signals were low-pass filtered at 9 kHz with eight-order Butterworth filters (–48 dB/octave) to prevent frequency aliasing. The cut-off frequency of 9 kHz was always greater than the PRF/2 used by the Doppler system, where PRF is the Pulse Repetition Frequency. During conversion, the use of sample and hold circuits simultaneously switched on assured that the phase relation-

ship between the quadrature Doppler signals was maintained. During Doppler signal acquisition, an algorithm for QRS detection was used to locate the beginning of each cardiac cycle and synchronize the analysis of the Doppler signals. The mean heart rate was also computed and used to reject all beats with an interval differing by more than 10% from the mean heart rate duration.

A Hanning window of 10 ms was applied to the Doppler signals and the Fast-Fourier Transform (FFT) algorithm used to compute a 256-sample power spectrum. By sliding the Hanning window over a period of 700 ms after the R-wave of the ECG with an increment of 5 ms between FFT computations, a Doppler spectrogram composed of 140 power spectra was produced. Finally, a mean power spectrogram was obtained by averaging, in synchronization with the R-wave of the ECG, 5 power spectrograms from a series of cardiac cycles. A typical mean power spectrogram of a normal patient is presented in Fig. 1.

Minimum and maximum frequency contour estimation

The minimum (F_{min}) and maximum (F_{max}) frequency contours of the mean spectrogram were estimated using a percentile method (Mo *et al.* 1988). Based on this method, F_{min} and F_{max} were defined respectively as frequencies where 10% and 90% of the integrated Doppler power spectrum was found. Since the percentile method is not adaptive to the noise level and signal bandwidth, it was applied only to spectra containing significant blood flow signal. On spectra containing pure noise, F_{min} and F_{max} were both set to the wall filter frequency (100 Hz). To determine which spectra of the spectrogram contain blood flow signal and which contain only pure noise, an objective and adaptive algorithm ("signal vs. noise" decision) was developed.

The adaptive algorithm was based on the fact that a spectrogram could be treated as an image on which a bidirectional threshold could be applied. The optimal values of the threshold were obtained by an iterative evaluation of the variability of the maximum frequency contour. The first step of the algorithm was the estimation of the background noise level of each spectrum and of the whole spectrogram, noted N_o and N_i , respectively. The mean amplitude of each power spectrum noted S_o was also computed. The value of N_o was obtained for each positive frequency spectrum (forward blood flow) by averaging the amplitude of the samples located at PRF/2 and PRF/2 minus one sample. For negative frequency spectra (reverse blood flow), samples located at –PRF/2 and –PRF/2 plus one sample were used. The value of N_i was obtained

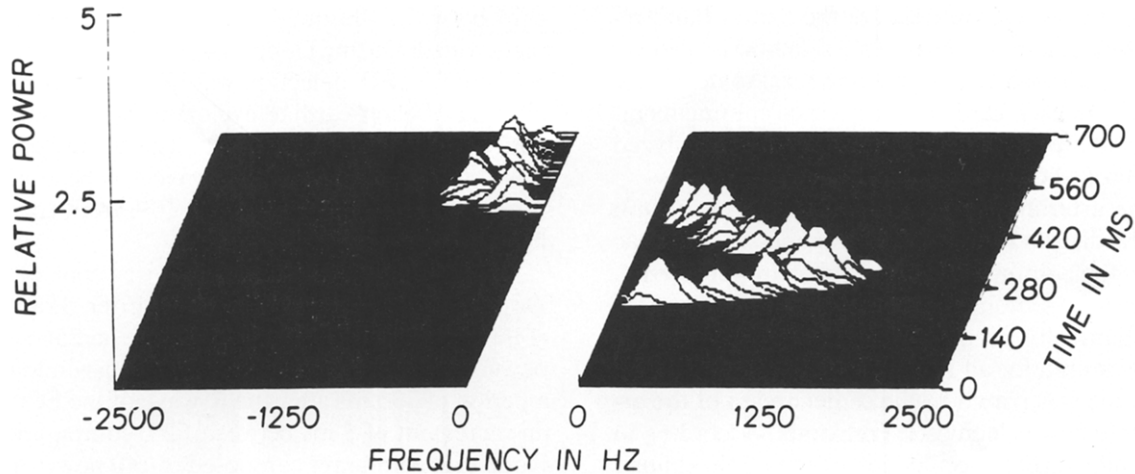


Fig. 1. Typical mean power spectrogram of a normal patient. The negative frequencies are associated with the reverse blood flow while the positive frequencies are associated with the forward blood flow.

by averaging the amplitude of the samples of all 140 spectra of the spectrogram located at $\pm\text{PRF}/2$ and $\pm(\text{PRF}/2-1)$. These frequency samples were also used to compute the coefficient of variation of the statistical distribution of the background noise. This statistical descriptor was obtained by dividing the standard deviation (σ) by the mean value of the background noise level of the spectrogram (N_t).

To assume that a given power spectrum contained significant Doppler blood flow signal, that spectrum had to fulfill one of the two following conditions: (1) its mean amplitude S_o had to be greater than some multiple of the mean background noise of the spectrogram N_t or (2) its background noise N_o had to be greater than some multiple of N_t . The first condition is associated with the signal-to-noise ratio of the power spectrum. The second is used to detect spectrum characterized by frequency aliasing. The occurrence of frequency aliasing means that significant Doppler blood flow is present. Defining W_s and W_n as two threshold parameters, the bidirectional threshold algorithm can be expressed as:
if

$$(S_o > W_s N_t)$$

or if

$$(N_o > W_n N_t),$$

then the spectrum contains blood flow signal; else the spectrum is mainly composed of noise.

In order to objectively determine which values of W_s and W_n lead to optimal signal detection, the variability of the maximum frequency contour of the

Doppler spectrogram was evaluated with different values of W_s and W_n . The optimal values of W_s and W_n were obtained when the variability of the maximum frequency contour reached a minimum. As demonstrated by Cloutier et al. (1990), optimal signal detection is obtained when the maximum frequency contour of the spectrogram shows minimum variability. The evaluation of the variability of the maximum frequency contour was limited to the positive component of the spectrogram since the negative component containing valuable information is found only in normal arteries or those with mild and moderate stenoses. Using FFT, an index of variability named IVAR (Cloutier et al. 1990) describing the variability of the maximum frequency contour was computed according to the following eqn:

$$\text{IVAR} = 100 \times \frac{\sum_i X(i)}{\sum_j X(j)} \quad \begin{array}{l} \text{NFFT}/4 < i \leq \text{NFFT}/2 \\ 0 < j \leq \text{NFFT}/2 \end{array} \quad (1)$$

where $X(i)$ and $X(j)$ denote the amplitudes of the FFT coefficients and NFFT, the number of samples (after zero-padding) of the maximum frequency contour, chosen to be equal to 256. In order to eliminate the indetermination when frequency contours were represented by a constant value, the value of IVAR for these specific cases was set to 100.

The same optimal values of W_s and W_n that were used for the positive component of the spectrogram were also used for the negative one. However, since reverse flow, when present, occurs only during diastole, the application of the "signal vs. noise" decision

algorithm was limited to that specific interval. The diastolic interval was defined as the interval following the peak systole and beginning at the time where the maximum positive frequency reaches the wall filter value. The end of the diastolic interval coincides with the end of the portion of the cardiac cycle analyzed (700 ms after the R-wave of the ECG). Before the diastolic interval, F_{min} and F_{max} of the negative component of the spectrogram were set to the wall filter frequency.

Feature extraction

A total of 19 raw diagnostic features were extracted from the negative (reverse flow) and positive (forward flow) components of the mean Doppler spectrogram of each patient. All features were extracted within the spectral envelope delimited by the minimum and maximum frequency contours. Since some features were related to the amplitude distributions, the amplitude of all samples located outside the spectral envelope was set to zero.

A description of all the features extracted from the mean spectrograms is given in Table 1. MXFS, MEFS, and MNFS are respectively the maximum, mean and minimum frequencies at peak systole. MXFD is the maximum negative frequency during diastole. SEAP and SEAN are, respectively, the spectral envelope area (Cannon *et al.* 1982) of the positive and negative frequencies. These features (expressed in kHz-s) are defined as the area of the positive and negative mean spectrograms delimited by the minimum and maximum frequency contours. AVGMXF is the time-averaged frequency of the maximum positive frequency contour. SBI is the spectral broadening index (Kassam *et al.* 1982) at peak systole. CV is the coefficient of variation of the frequency distribution at peak systole (Kalman *et al.* 1985). The 10 following features in Table 1 are associated with the amplitude of the power spectrogram within various (positive and negative) frequency bands. Since the amplitude of the Doppler blood flow signals may be attenuated in different ways from one patient to another and from one site to another, normalized amplitudes of the power spectrogram should be considered. The latter were computed as follows:

$$A_{ij} = \frac{\frac{1}{N_{ij}} \sum_{t=0}^T \sum_{f=i}^j X(t, f)}{\frac{1}{N_{WF}} \sum_{t=0}^T \sum_{f=W}^F X(t, f)} \quad (2)$$

where A_{ij} represents the normalized amplitude of the power spectrogram within the i to j frequency band, $X(t, f)$ the amplitude of the power spectrogram at time t and at frequency f , N_{ij} and N_{WF} the number of

Table 1. Description of the diagnostic features.

Features	Description
Frequency Features:	
MXFS:	maximum positive frequency @ peak systole (kHz)
MEFS:	mean positive frequency @ peak systole (kHz)
MNFS:	minimum positive frequency @ peak systole (kHz)
MXFD:	maximum negative frequency @ diastole (kHz)
SEAP:	spectral envelope area of the positive frequencies (kHz-s)
SEAN:	spectral envelope area of the negative frequencies (kHz-s)
AVGMXF:	time-averaged frequency of the maximum positive frequencies (kHz)
SBI:	spectral broadening index @ peak systole
CV:	coefficient of variation of the frequency distribution @ peak systole
Amplitude Features:	
A1213:	normalized amplitude in the 100–1000 Hz positive frequency band*
A1333:	normalized amplitude in the 1000–3000 Hz positive frequency band*
A3353:	normalized amplitude in the 3000–5000 Hz positive frequency band*
A5383:	normalized amplitude in the 5000–8000 Hz positive frequency band*
A1223:	normalized amplitude in the 100–2000 Hz positive frequency band*
A2343:	normalized amplitude in the 2000–4000 Hz positive frequency band*
A4383:	normalized amplitude in the 4000–8000 Hz positive frequency band*
B1252:	normalized amplitude in the 100–500 Hz negative frequency band*
B1213:	normalized amplitude in the 100–1000 Hz negative frequency band*
B1223:	normalized amplitude in the 100–2000 Hz negative frequency band*

* These frequency band values are those before frequency scaling.

samples having a nonzero amplitude and included in the i to j and in the W to F frequency band, respectively. Parameter W is the wall filter frequency (100 Hz) and parameter F is the sampling rate (20 kHz) divided by two. T is the duration of the portion of the cardiac cycle analyzed (700 ms). The frequency bands considered included the following frequencies: 100, 500, 1000, 2000, 3000, 4000, 5000 and 8000 Hz. As explained in the next section, the frequency bands delimited by these frequencies were scaled according to the site investigated in order to compensate blood flow velocity variations from site to site.

Frequency band and frequency feature scaling

It is well known that, in healthy subjects, blood flow velocity varies significantly from the aorta to the

popliteal artery (Jager et al. 1985). These velocity variations require the design of a specific classifier for each arterial segment in order to optimize the performance of the pattern recognition system. The disadvantage of this approach, however, is that the total population size is subdivided into smaller subgroups which will inevitably reduce the reliability of the pattern recognition system. Until a much larger training set is accumulated in each segment, it was decided to compensate the velocity variations from site to site by using a frequency scaling factor to design a single classifier for all the segments investigated. A frequency scaling factor was defined for each site and applied to all features which were frequency-dependent regardless of the presence of stenoses on the artery investigated. The frequency scaling factors were defined so that, at each site, the mean value of the maximal frequency at peak systole for all normal (0% diameter reduction) arteries became identical.

The following procedure was used to compute the different values of the frequency scaling factor. In a preliminary step, the maximum frequency at peak systole MXFS of each normal artery was determined from the maximum frequency contours. For each site number "*i*" described in Table 2, a mean maximum frequency at peak systole MMXFS[*i*] was computed by averaging the corresponding MXFS values of all normal arteries. The MMXFS[*i*] values were then used to calculate a frequency scaling coefficient FSC[*i*] according to the following eqn:

$$FSC[i] = MMXFS[S]/MMXFS[i] \quad (3)$$

where MMXFS[*S*] is the smallest value among all the MMXFS[*i*] values. This means that the FSC[*S*] is equal to 1 since the MMXFS[*S*] was arbitrarily chosen as reference to define the FSC[*i*] values. All frequency features of Table 1, except SBI and CV which are frequency ratio, were scaled by multiplying them by their corresponding frequency scaling factors. The frequency bands within which the normalized ampli-

Table 2. Mean maximum frequency at peak systole (MMXFS[*i*]) of 273 normal segments and frequency scaling coefficients (FSC[*i*]) used for frequency scaling of features.

Arterial segment	<i>i</i>	<i>N</i>	MMXFS[<i>i</i>] (kHz)	FSC[<i>i</i>]
Aorta	1	25	1419	1.00
Common iliac	2	34	2192	0.65
External iliac	3	40	2246	0.63
Common femoral	4	51	3119	0.45
Profunda femoral	5	49	2358	0.60
Superficial femoral	6	23	2486	0.57
Popliteal	7	50	1546	0.92

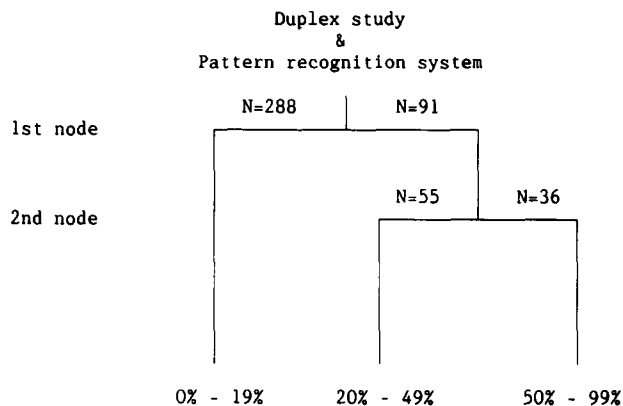


Fig. 2. Classification scheme I. At the first node, the algorithm separated normal and mildly diseased vessels (0–19%) from those with moderate and severe disease (20–99%) and, at the second node, it separated moderate (20–49%) from severe (50–99%) stenoses.

tude features were computed, as listed in Table 1, were also scaled.

Classifier design and evaluation

The computerized classification of arterial stenoses into two or more classes can be achieved by using a computer-based pattern recognition approach. Various techniques for designing and evaluating a pattern recognition system have been described in the literature (Jain 1987; Tou and Gonzalez 1974; Tous-saint 1974). A classifier using a three-class supervised learning algorithm based on the Bayes' rule was developed for the present study. A similar classifier has already been used in our laboratory for the classification of bioprosthetic heart valve degeneration (Durand et al. 1990). The Bayes classifier is one of the most popular parametric approaches and also an optimal one when the probability density function of the patterns (ensemble of features) is known and belongs to a parametric family. In the present study, we assumed that the probability density function of the patterns was Gaussian.

The pattern recognition system was designed to classify stenoses of the lower limb arteries into three categories: 0 to 19% diameter reduction, 20 to 49% diameter reduction and 50 to 99% diameter reduction. Two classification schemes using a two-node decision rule were tested as shown in Figs. 2 and 3. The first scheme was designed to separate, at the first node, normal and mildly diseased vessels (0–19%) from those with moderate and severe disease (20–99%), and, at a second node, to separate moderate (20–49%) from severe (50–99%) stenoses. The second scheme was designed to separate, at the first node, nonhemodynamically significant (0–49%) from hemodynamically

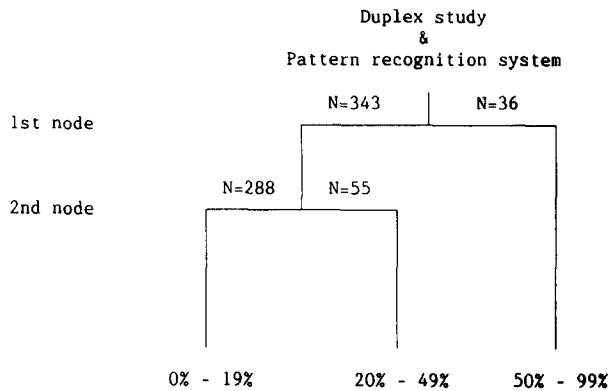


Fig. 3. Classification scheme II. At the first node, the algorithm separated nonhemodynamically significant (0–49%) from hemodynamically significant (50–99%) stenoses and, at the second node, it separated normal and mildly diseased vessels (0–19%) from those with moderate disease (20–49%).

cally significant (50–99%) stenoses and, at the second node, normal and mildly diseased vessels (0–19%) from those with moderate disease (20–49%).

All features described in Table 1 were considered to have potential discriminant power. However, only subsets of this ensemble of features were tested in order to maintain a ratio of the sample size per class to the feature size (N/L) greater than 5. This minimum ratio has been recommended in the past to minimize the risk of overestimating the real performance of the classifier (Foley 1972; Trunk 1979; Kalayeh and Landgrebe 1983; Jain 1987). The approach used in the present study to determine which feature subset gave the best results was to test, at each node, all possible feature subsets of size p varying between one and $N/5$, where N was the smallest training sample size in a class for a specific node. The algorithm used to design the pattern recognition system ran on a SUN-4 computer.

Conventional biplane contrast angiographic studies, used as a gold standard reference, were performed on all patients to evaluate the performance of the classifiers. Each angiographic film was read by an experienced angiologist, and the degree of maximum arterial stenosis in each separate segment was assessed by caliper measurements of the arteriograms. Neither the angiologist nor the technologist performing the noninvasive studies were aware of each other's results.

The performance of the classifier to discriminate between the predefined categories of disease was evaluated with the leave-one-out method (Toussaint 1974). In this iterative method, the training set is composed of the complete population minus one sample while the test set is formed by the excluded sample. At each

iteration, a new sample is used to form the test set. When each sample has been classified, the performance of the classifier is evaluated by expressing, in percentage, the number of correct classifications (CC). Sensitivity (SE), specificity (SP), positive predictive value (PPV) and negative predictive value (NPV) were also computed (Feinstein 1977). Although it requires a larger amount of computation time, the leave-one-out method was used because it is characterized by a small bias (Toussaint 1974). Finally, to take into account the fact that the disease distribution was not homogeneous, we computed the Kappa statistic, a chance-corrected measure of agreement between two observations (Cohen 1960).

RESULTS

In this study, 37 patients with a mean age of 58 ± 15 years (range of 21 to 79 years) were evaluated by ultrasonic duplex scanning and arteriography. This population provided a total of 481 lower limb arterial segments available for study. A total of 102 segments were not included in the computer analysis for the following reasons: (1) 10 segments could not be studied by angiography, (2) 6 segments (1 side) could not be used due to prior bypass graft surgery, (3) 11 segments could not be digitized because of electronic failure of the ECG recording system, (4) 6 segments were not analyzed because of cardiac arrhythmias, (5) 27 segments were not adequately recorded by the technologist, (6) 16 (primitive or external) iliac segments were missing because initially the protocol for data acquisition included only one recording for this segment, and (7) 24 segments were occluded (no Doppler signals) according to the technologist. The occlusions diagnosed in 22 segments by arteriography were recognized by the noninvasive technologist in 95% (21/22) of the cases and only 3 of the 382 patent segments (0.8%) were wrongly classified as occlusions (Table 3).

Among the 379 segments available for the computer analysis, 288 (76%) presented a 0 to 19% diame-

Table 3. Comparison of angiography to duplex scanning (visual interpretation) in detecting arterial occlusions.

		Duplex classification		
		0%–99%	100%	Total
Angiography	0%–99%	379	3	382
	100%	1	21	22
	Total	380	24	404

Accuracy = 99%; sensitivity = 95%; specificity = 99%; positive predictive value = 88%; negative predictive value = 100%.

ter reduction (51 were from young presumed normal volunteers which were not subjected to arteriography, mean age = 25), 55 (15%) segments had a 20 to 49% lesion, and 36 (9%) had a 50 to 99% lesion. Among the latter, 23 are associated with the presence of severe disease (50–100%) in other adjacent (proximal and/or distal) segments.

Table 2 shows the mean maximum frequency at peak systole for each group of normal arteries as determined from the maximum frequency contours. The frequency scaling coefficient for each site is also presented. As shown in Table 2, the aorta has a frequency scaling coefficient of 1 while the common femoral has a FSC of only 0.45 since the greatest velocities are found in this site. This means that frequency-dependent features and frequency bands of amplitude features extracted from the aorta were unscaled while those extracted from the common femoral were scaled by a factor of 0.45.

For the 379 arterial segments included in this study, the mean value of the coefficient of variation of the statistical distribution of the background noise was 2.65 ± 1.55 (range of 0.46 to 8.86). This large mean value indicates that the amplitude of the samples located close to $\pm PRF/2$ varies greatly within a given spectrogram. Moreover, the coefficient of variation (CV) also greatly varies from one spectrogram to another, as indicated by the large standard deviation of 1.55. According to the definition of CV described earlier, this statistical parameter represents a normalized measure of the spread of the distribution of the amplitude of the background noise N_o around its mean value N_t . Since the CV has a large mean value (2.65), this means that the value of the standard deviation of the N_o values is greater than N_t . As a result, the shape of the distribution of the N_o values around N_t has an asymmetric tail extending out towards larger N_o values. This could be explained in some situations by the occurrence of frequency aliasing since, in these cases, frequency samples located at $PRF/2$ are associated with blood flow.

These statistical considerations were used to set the boundaries of the W_n threshold, which detected spectra characterized by frequency aliasing. It was decided that if the N_o value of a spectrum satisfied the following eqn:

$$\frac{N_o}{N_t} > CV + 1, \quad (4)$$

then it could contain significant Doppler blood flow components. In order to cover the wide range of $CV + 1$ observed in this analysis (1.46–9.86) and in further analysis, the minimum and maximum values of

W_n were set respectively to 1.5 and 12. The boundary values of the W_s threshold were set using the signal-to-noise ratio expected with commercial Doppler systems (range of about 10 to 23 dB or 10 to 200 in linear scale). The visual inspection of the frequency contours of the spectrograms has shown that five values of W_n (1.5, 3, 6, 9 and 12) and five values of W_s (10, 20, 40, 100 and 200) were necessary to cover the different Doppler signal characteristics.

To determine which bidirectional threshold values lead to optimal signal detection, IVAR of the maximum frequency contour of 379 Doppler spectrograms was computed for each combination of W_n and W_s . For each combination, a mean IVAR was also computed. With this global approach, it was found that no specific values of the bidirectional threshold could significantly minimize the mean IVAR as shown in Table 4 (left columns). Moreover, the variability of the IVAR values was in some cases quite large. The analysis of these results suggested that the use of an individual approach could provide a

Table 4. The left part of the table showed, for each combination of W_s and W_n , the mean value of the index of variability (IVAR) of the maximum positive frequency contour of the 379 spectrograms. The mean optical value of the index of variability ($IVAR_{opt}$) obtained using the iterative procedure and its distribution according to W_s and W_n are presented in the last two columns.

W_s	W_n	IVAR \pm SD	N	$IVAR_{opt} \pm$ SD	N
10	1.5	18.8 \pm 12.1	379	11.2 \pm 4.2	103
	3	15.8 \pm 8.7	379	14.0 \pm 6.8	5
	6	15.6 \pm 8.4	379	—	0
	9	15.8 \pm 9.5	379	—	0
	12	16.0 \pm 9.8	379	—	0
20	1.5	18.6 \pm 12.2	379	9.5 \pm 4.3	45
	3	14.3 \pm 8.1	379	11.4 \pm 5.4	13
	6	14.1 \pm 8.0	379	20.2 \pm 2.5	2
	9	14.5 \pm 10.4	379	—	0
	12	14.9 \pm 11.4	379	—	0
40	1.5	19.3 \pm 12.1	379	9.8 \pm 3.1	40
	3	14.7 \pm 8.6	379	10.8 \pm 4.1	17
	6	14.6 \pm 8.9	379	14.1 \pm 1.5	3
	9	15.2 \pm 11.7	379	11.2 \pm 0	1
	12	15.7 \pm 12.9	379	—	0
100	1.5	20.2 \pm 12.2	379	9.6 \pm 2.8	44
	3	15.9 \pm 9.9	379	10.1 \pm 4.1	24
	6	16.2 \pm 11.2	379	7.8 \pm 1.6	4
	9	17.4 \pm 14.9	379	18.1 \pm 8.7	2
	12	18.3 \pm 16.8	379	—	0
200	1.5	21.1 \pm 12.1	379	9.8 \pm 2.4	39
	3	17.6 \pm 11.5	379	9.8 \pm 3.3	31
	6	18.3 \pm 13.9	379	14.5 \pm 1.4	4
	9	19.8 \pm 17.0	379	6.8 \pm 0	1
	12	21.2 \pm 19.9	379	33.8 \pm 0	1

The mean value of $IVAR_{opt} = 10.5 \pm 4.1$ for the 379 segments.

better estimation of the frequency contour of each spectrogram. This meant that, for each spectrogram, an iterative procedure had to be used to determine values of W_n and W_s which minimized IVAR. The minimum value of IVAR was named $IVAR_{opt}$. For the 379 arterial segments included in this study, the mean value of $IVAR_{opt}$ was 10.5 ± 4.1 (range of 4.6 to 33.8) which is significantly less than the mean IVAR values obtained with the global approach (minimum value of 14.1 ± 8.0 for $W_s = 20$ and $W_n = 6$). The value of the mean $IVAR_{opt}$ and its distribution according to W_n and W_s are presented in Table 4 (right columns). If $IVAR_{opt}$ was obtained with more than one combination of W_s and W_n , the one with the smallest W_s and W_n was chosen. Influences of the bidirectional threshold values on the maximum positive frequency contours are presented in Fig. 4. To illustrate the result obtained using the iterative bidirectional threshold algorithm, the minimum and maximum frequency contours of both the positive and negative components of the spectrogram of Fig. 1 are presented in Fig. 5.

The best results obtained by the pattern recognition system with the classification schemes I and II are shown in Tables 5 and 6, respectively. The most discriminant features used at each decision node by the pattern recognition system are also identified. No feature size greater than 7 was tested either to respect a sample size to feature size ratio greater than 5 or because it would have required a too large amount of computation time to test all possible feature subsets of size less than $N/5$ (where N is the smallest sample size in a class). Moreover, we observed that the performance of the classifier remains almost stable when the feature size increases from 4 to 7. In order to compare the results of the pattern recognition approach, the performance obtained by visual interpretation of the Doppler waveforms was tabulated and presented in Table 7. An accuracy of 76% was obtained which results in a Kappa value of 0.33 between the technologist and the angioradiologist. The criteria used to perform visual classification of the Doppler waveforms were those already defined by Jager *et al.* (1985).

The overall accuracy of the pattern recognition

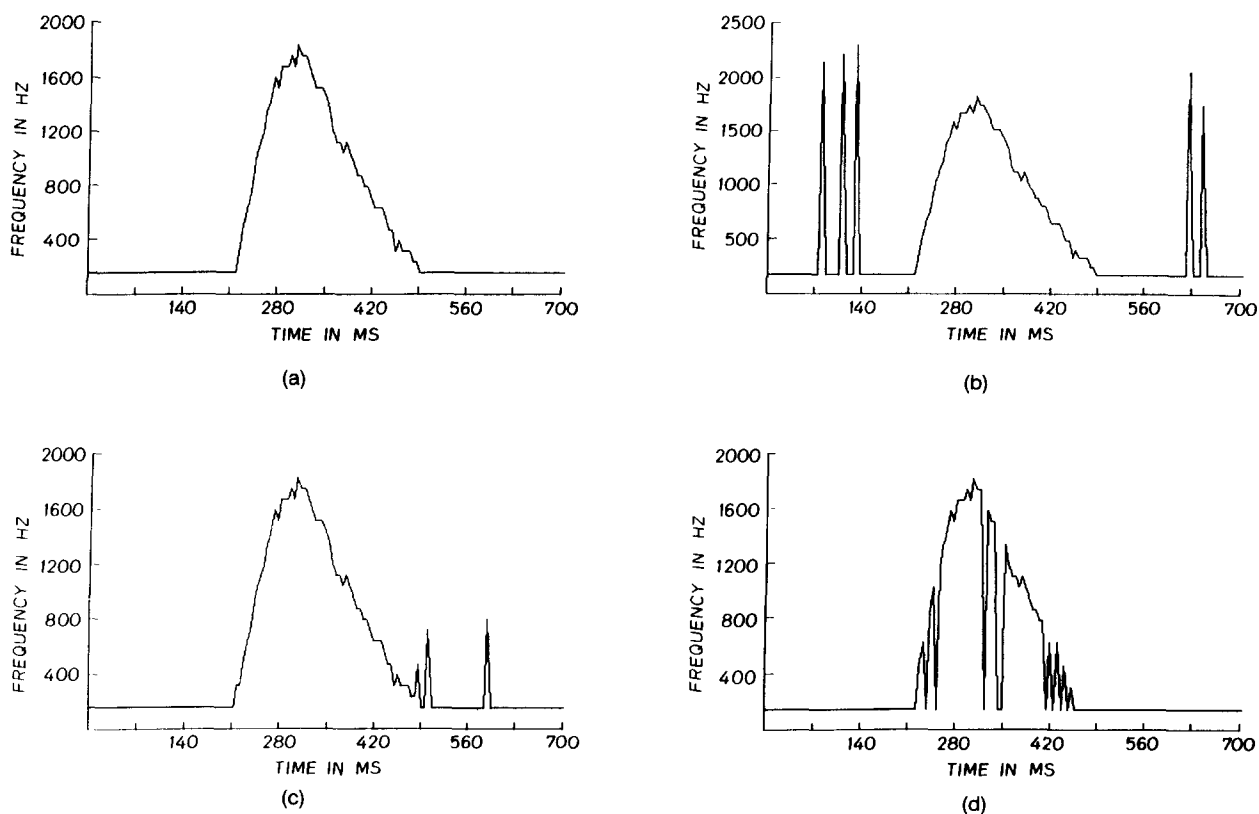


Fig. 4. Four examples showing the influences of the W_n and W_s threshold levels on the determination of maximum positive frequency contour. (a) Maximum positive frequency contour obtained using optimal values of W_s and W_n ($IVAR = 7.35$; $W_s = 20$; $W_n = 3$), (b) frequency contour obtained using too small a value of W_n ($IVAR = 38.0$; $W_s = 20$; $W_n = 1.5$), (c) frequency contour obtained using too small a value of W_s ($IVAR = 18.5$; $W_s = 10$; $W_n = 3$) and (d) frequency contour obtained using too large a value of W_s and of W_n ($IVAR = 7.5$; $W_s = 200$; $W_n = 6$).

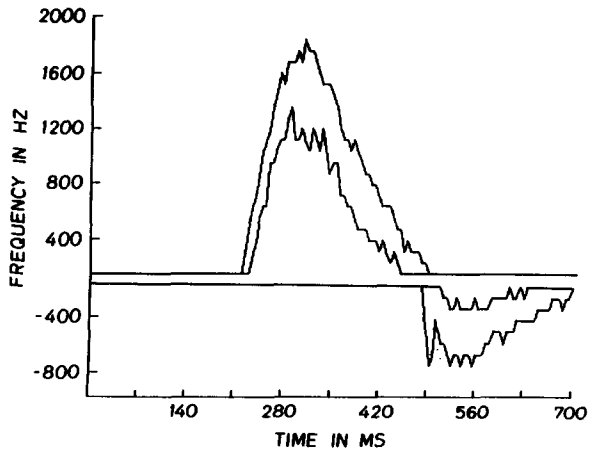


Fig. 5. Minimum and maximum frequency contours of both the positive and negative components of the spectrogram of Fig. 1 obtained by using optimal values of W_s and W_n .

using the classification scheme I was 83% (313/379), the Kappa value being 0.42. Thus, the agreement between the pattern recognition system and angiography was 83% (314/379) for the first decision node and 91% (31/34) for the second decision node. Of the 288 segments in the 0–19% class, 284 (99%) were correctly classified. Of the 55 segments in the 20–49% class, only 11 (20%) were correctly classified. Of the 36 segments in the 50–99% class, 18 (50%) were correctly classified.

With the classification scheme II, the overall accuracy of the pattern recognition was 81% (306/379), the Kappa value being 0.35. The agreement between the pattern recognition system and angiography was 93% (354/379) for the first decision node and 81% (288/354) for the second decision node. Of the 379 segments in the 0–19% class, 283 (98%) were correctly classified. Of the 55 segments in the 20–49% class, only 5 (9%) were correctly classified. Of the 36 segments in the 50–99% class, 18 (50%) were correctly classified.

Comparison of Tables 5, 6 and 7 shows that the pattern recognition method is much better than the technologist's approach to detect normal and mildly diseased arteries.

DISCUSSION

Data acquisition and analysis

It is well recognized that the acquisition of optimal Doppler blood flow signals is a crucial step prior to diagnostic feature extraction and waveform classification. For example, Baker et al. (1989) have reported that the performance of the Laplace transform analy-

Table 5. Comparison of angiography to pattern recognition of Doppler blood flow in detecting arterial disease using classification scheme I.

	Pattern recognition classification				
	0%–19%	20%–49%	50%–99%	Total	
Angiography	0%–19%	284	2	2	288
	20%–49%	44	11	0	55
	50%–99%	17	1	18	36
Total	345	14	20	379	

Accuracy = 83%; Kappa = 0.42.

Most discriminant features at the first node: MEFS A1323 A3343 FMXD B1252.

Most discriminant features at the second node: SBI A1252 A3343 B1252.

sis was very sensitive to the quality of recorded signals. Interobserver and intraobserver variability in the measurement of Doppler blood flow signal features has also been reported by Kohler et al. (1987b). For these reasons, a standard examination technique was used for all patients in order to obtain reliable Doppler signals for disease classification. For instance, care was taken to place the sample volume in the centerstream of the artery, as indicated on the B-mode image. However, since patients were not asked to fast before examination, abdominal gas was sometimes the cause of interference which prevented optimal recording of characteristic Doppler signals of some segments. All examinations were finally performed at a fixed angle approaching to 60 degrees (58.9 ± 3.6 degrees) between the Doppler beam and the vessel axis. Even though some arteries were better visualized using a slightly different angle, no angle adjustment was applied on frequency features to compensate for these variations. The reason is that angle adjustment is appropriated only when blood flow is parallel to the vessel axis (Beach et al. 1989). When

Table 6. Comparison of angiography to pattern recognition of Doppler blood flow in detecting arterial disease using classification scheme II.

	Pattern recognition classification				
	0%–19%	20%–49%	50%–99%	Total	
Angiography	0%–19%	283	4	1	288
	20%–49%	44	5	6	55
	50%–99%	18	0	18	36
Total	345	9	25	379	

Accuracy = 81%; Kappa = 0.35.

Most discriminant features at the first node: AVGMXF A2333 A3343 SEAN B1252.

Most discriminant features at the second node: MEFS B1252.

Table 7. Comparison of angiography to duplex scanning (visual interpretation) in detecting arterial disease.

		Duplex classification			Total
		0%–19%	20%–49%	50%–99%	
Angiography	0%–19%	265	21	2	288
	20%–49%	43	7	5	55
	50%–99%	13	5	18	36
	Total	321	33	25	379

Accuracy = 76%; Kappa = 0.33.

this latter is not parallel to the vessel axis, angle adjustment could lead to significant errors in the estimation of the blood flow velocity.

The number of heartbeats suitable for the spectral averaging still remains an empirical choice. Since no studies to date have defined the best suited number of cardiac cycles required to significantly reduce spectrogram variability, we considered that spectrogram averaging using five cardiac cycles was an acceptable choice.

To obviate the major limitation of the percentile method (as noted by Mo *et al.* 1988) in the estimation of the frequency contours, a bidirectional threshold algorithm was developed. This algorithm allowed the determination of spectra of the spectrogram containing blood flow signal and of those containing only pure noise. The algorithm was based on the estimation of the background noise level by using the amplitude of the samples located close to $\pm PRF/2$. A difficulty was to determine the values of the bidirectional threshold because the amplitude of the samples close to $\pm PRF/2$ showed a large variability (mean value of the coefficient of variation = 2.65 ± 1.55). Compared to the same statistical parameter computed by Cloutier *et al.* (1990) for cardiac blood flow signals, our mean value for the coefficient of variation was greater by a factor of about three. We initially attempted to explain this variability by the presence of frequency aliasing, but visual inspection of the spectrograms revealed that very few of them disclosed this feature. The large variability of the amplitude of the samples close to $\pm PRF/2$ prevented the use of a frequency contour estimation algorithm based on a fixed threshold level because this could lead to erratic frequency contours. The computation of the frequency contour variability under different bidirectional threshold values allowed the determination of the frequency contours of almost all spectrograms with accuracy. This was demonstrated by the fact that the variability of the frequency contour obtained using such an iterative procedure was much less than the variability ob-

tained using a predetermined bidirectional threshold level.

Although our approach based on the iterative evaluation of the variability of the frequency contour of each spectrogram under different threshold values was tested only with the percentile method, we believe that it would also significantly improve the effectiveness of the modified threshold method and the hybrid method (Cloutier *et al.* 1990; Mo *et al.* 1988). Indeed, the threshold value used in these two methods could be optimally determined according to the signal characteristics by the iterative approach proposed.

Pattern recognition

No results obtained by a pattern recognition system to classify lower limb arterial stenoses have been published so far. The only instance in which a pattern recognition approach has been used in vascular disease classification was for the evaluation of carotid artery stenoses (Langlois *et al.* 1984). The results of Langlois *et al.* showed an overall accuracy of 83% (Kappa = 0.77) for the classification of 170 carotid lesions into four categories of disease. By using two different classification schemes to classify disease of 379 lower limb arterial segments into three classes instead of four, we obtained an overall accuracy of 83% (Kappa = 0.42) with classification scheme I and 81% (Kappa = 0.35) with classification scheme II. For the 379 segments, visual interpretation showed an accuracy of 76% (Kappa = 0.33). These results indicated that the pattern recognition approach allows a better discrimination than visual interpretation, especially for the 0 to 19% lesion and also for the 20–49% lesion when using classification scheme I.

The need to differentiate hemodynamically significant (50–99%) from nonhemodynamically significant (0–49%) stenosis is clinically obvious. The performance of the classifier to make this distinction is disappointing and no better than the one obtained by visual interpretation. The pattern recognition system using classification scheme I yields a sensitivity and a specificity of 50% and 99%, respectively. With classification scheme II, the sensitivity and the specificity are 50% and 98%, respectively. The 18 diseased (50–99%) segments that were misclassified using classification scheme I were also misclassified using scheme II. Our results were greatly affected by multisegmental disease. Indeed, among the 23 diseased segments associated to the presence of 50–100% diameter reduction lesions in other adjacent (proximal and/or distal) segments, misclassification occurred in 15 segments. Among the 13 diseased segments associated to unisegmental disease, misclassification occurred in only 3 segments. This finding underlines the fact that con-

sidering segmental disease independently of lesions in other segments constitutes a limitation of our pattern recognition system to study lower limb arteries. With increase in the representation of moderate and severe lesions, it will be possible to design a classifier that will take into account neighboring lesions and thus obviate these problems.

We also think that the poor sensitivity of the pattern recognition system to detect moderate and severe stenoses can be explained by the skewness of the distribution of disease towards normal segments (273 of 379 segments). This nonhomogeneous distribution found in our population causes the classifier to underestimate the extent of disease, as indicated by the very high specificity of the classifier. Skewness of the distribution of disease should foster us to use classification scheme I where normal and minimal lesions are first separated from moderate and severe lesions ($\geq 20\%$). The second node decision will thus be more significant. It should also be mentioned that the results presented in this study were those obtained by using the percentage of correct classification as the criterion to decide which feature subset leads to the best performance of the classifier. No receiver operating characteristic (ROC) curves were generated from the classifier to obtain a better compromise between sensitivity and specificity.

Finally, when comparing the agreement between Doppler waveform classification and angiography, one should be aware of the limitations of angiography as a "gold standard reference" (Thiele and Strandness 1983). Although we anticipated a better correlation between pulsed Doppler and angiography, it remains that perfect agreement should not be expected since arteriography provides anatomic rather than hemodynamic information. Furthermore, intraobserver and interobserver variability exists in the reading of angiograms even when broader classifications of disease are used. For instance, when classifying the degree of lower limb arterial disease into five categories, it has been reported (Jager et al. 1985) that the agreement between two angioradiologists reading independently the same film is only 70% ($Kappa = 0.63$).

CONCLUSION

A new algorithm to estimate the frequency contours of Doppler spectrograms of blood flow in the lower limb arteries is presented. The algorithm is based on a percentile method improved by the use of a bidirectional threshold whose optimal values were determined by an iterative evaluation of the variability of the positive frequency contour. The advantage of this algorithm resides in its high degree of adaptiv-

ity to the variability of the Doppler signals over a cardiac cycle, thus allowing estimation of frequency contours with reliability.

A Bayes classifier was developed to classify lower limb arterial stenoses into three categories of disease. An important characteristic is that the same classifier was used to evaluate the different segments in 379 arteries, starting from the aorta down to the popliteal artery. A frequency scaling procedure was performed to take into account differences in blood flow velocities observed between sites. The overall performance of our pattern recognition approach is comparable to the one obtained by Langlois et al. (1984) for the evaluation of carotid artery stenoses. Although the specificity of our classifier for lower limb disease is very high, its sensitivity needs to be improved. To obtain a better compromise between sensitivity and specificity, it would be necessary to generate receiver operating characteristic (ROC) curves from the classifier. Indeed, the results presented in this study were obtained using the percentage of correct classification as the criterion to decide which feature subset leads to the best performance of the classifier, and no compromise between sensitivity and specificity was searched for. Another improvement for the future would be the integration into the classifier of information related to the multilevel disease cases. Compared to the carotid artery, the characterization of blood flow patterns in lower limb arteries is more complex, which will inevitably lead to the design of a specific classifier for each site. Such a realization will be possible as our population size increases (especially the 50–99% lesion). New areas of investigation will also be directed towards the evaluation of a classifier based on distance measurement (like nearest neighbor method) instead of on probability estimation (like the Bayes rule). We finally expect that the use of a color-flow duplex imaging in a near future will allow us to obtain Doppler signals with more reliability and also to reduce examination time.

Acknowledgment—The authors wish to acknowledge Mr. Michel Blanchard for the development of the pattern recognition program. This research was supported by the Medical Research Council of Canada for grant support (Grant #MA-10030) and the Monat Foundation.

REFERENCES

- Baker, J. D.; Machleder, H. I.; Skidmore, R. Analysis of femoral artery Doppler signals by LaPlace transform damping method. *J. Vasc. Surg.* 1:520–524; 1984.
- Baker, J. D.; Skidmore, R.; Cole, S. E. A. LaPlace transform analysis of femoral artery Doppler signals: The state of the art. *Ultrasound Med. Biol.* 15:13–20; 1989.
- Beach, K. W.; Lawrence, R.; Phillips, D. J.; Primozich, J.; Strandness D. E., Jr. The systolic velocity criterion for diagnosing sig-

- nificant internal carotid artery stenoses. *J. Vasc. Tech.* 13:65–68; 1989.
- Cannon, S. R.; Richards, K. L.; Rollwitz, W. T. Digital Fourier techniques in the diagnosis and quantification of aortic stenosis with pulsed-Doppler echocardiography. *J. Clin. Ultrasound* 10:101–107; 1982.
- Cloutier, G.; Lemire, F.; Durand, L. G.; Latour, Y.; Jarry, M.; Solignac, A.; Allard, L.; Langlois, Y. E. Characterization of spectral broadening of Doppler signals recorded in the left ventricular outflow tract of patients with a valvular aortic stenosis. *Proc. IEEE Eng. in Med. & Biol.* 11:67–68; 1989.
- Cloutier, G.; Lemire, F.; Durand, L. G.; Latour, Y.; Langlois, Y. E. Computer evaluation of Doppler spectral envelope area in patients having a valvular aortic stenosis. *Ultrasound Med. Biol.* 16:247–260; 1990.
- Cohen, J. A coefficient of agreement for nominal scales. *Educational and Psychological Measurement* XX:37–46; 1960.
- Durand, L.-G.; Blanchard, M.; Cloutier, G.; Sabbah, H. N.; Stein, P. D. Comparison of pattern recognition methods for computer assisted classification of spectra of heart sounds in patients with a porcine bioprosthetic valve implanted in the mitral position. *IEEE Trans. Biomed. Eng.* 37:1121–1129; 1990.
- Evans, D. H.; Barrie, W. W.; Asher, M. J.; Bentley, S.; Bell, P. R. F. The relationship between ultrasonic pulsatility index and proximal arterial stenosis in a canine model. *Circ. Res.* 46:470–475; 1980.
- Feinstein, A. R. On the sensitivity, specificity and discrimination of diagnostic tests. *Clinical biostatistics*. Saint Louis, MO: C. V. Mosby Company; 1977:214–226.
- Foley, D. H. Consideration of sample and feature size. *IEEE Trans. Info. Theory* 18:618–626; 1972.
- Gosling, R. G.; Dunbar, G.; King, D. H.; Newman, D. L.; Side, C. D.; Woodcock, J. P.; Fitzgerald, D. E.; Keates, J. S.; MacMillan, D. The quantitative analysis of occlusive peripheral arterial disease by a noninvasive ultrasonic technique. *Angiology* 22:52–55; 1971.
- Greene, F. M., Jr.; Beach, K.; Strandness D. E., Jr.; Fell, G.; Phillips, D. J. Computer based pattern recognition of carotid arterial disease using pulsed Doppler ultrasound. *Ultrasound Med. Biol.* 8:161–176; 1982.
- Hutchinson, K. J.; Karpinski, E. Stability of flow pattern in the *in vivo* post-stenotic velocity field. *Ultrasound Med. Biol.* 14:269–275; 1988.
- Jager, K. A.; Phillips, D. J.; Martin, R. L.; Hanson, C.; Roederer, G. O.; Langlois, Y. E.; Ricketts, H. J.; Strandness, D. E., Jr. Noninvasive mapping of lower limb arterial lesions. *Ultrasound Med. Biol.* 11:515–521; 1985.
- Jain, A. K. Advances in statistical pattern recognition. In: *Pattern recognition theory and applications*. F30. Berlin: Springer-Verlag; 1987:1–19.
- Johnston, K. W.; Kassam, M.; Cobbold, R. S. C. Relationship between Doppler pulsatility index and direct femoral pressure measurements in the diagnosis of aortoiliac occlusive disease. *Ultrasound Med. Biol.* 9:271–281; 1983.
- Johnston, K. W.; Kassam, M.; Koers, J.; Cobbold, R. S. C. Comparative study of four methods for quantifying Doppler ultrasound waveforms from the femoral artery. *Ultrasound Med. Biol.* 10:1–12; 1984.
- Kalayeh, M. M.; Landgrebe, D. A. Predicting the required number of training samples. *IEEE Trans. PAMI* 5:664–667; 1983.
- Kalman, P. G.; Johnston, K. W.; Zuech, P.; Kassam, M.; Poots, K. *In vitro* comparison of alternative methods for quantifying the severity of Doppler spectral broadening for the diagnosis of carotid arterial occlusion disease. *Ultrasound Med. Biol.* 11:435–440; 1985.
- Kassam, M. S.; Cobbold, R. S. C.; Johnston, K. W.; Graham, C. M. Method for estimating the Doppler mean velocity waveform. *Ultrasound Med. Biol.* 8:537–544; 1982.
- Kohler, T. R.; Nance, D. R.; Cramer, M. M.; Vandenburghe, N.; Strandness, D. E., Jr. Duplex scanning for diagnostic of aortoiliac and femoropopliteal disease: A prospective study. *Circulation* 76:1074–1080; 1987a.
- Kohler, T. R.; Langlois, Y.; Roederer, G. O.; Phillips, D. J.; Beach, K. W.; Primozich, J.; Lawrence, R.; Nicholls, S. C.; Strandness, D. E., Jr. Variability in measurement of specific parameters for carotid duplex examination. *Ultrasound Med. Biol.* 13:637–642; 1987b.
- Langlois, Y. E.; Greene F. M., Jr.; Roederer, G. O.; Jager, K. A.; Phillips, D. J.; Beach, K. W.; Strandness, D. E., Jr. Computer based pattern recognition of carotid artery Doppler signals for disease classification: Prospective validation. *Ultrasound Med. Biol.* 10:581–595; 1984.
- Langsfeld, M.; Nepute, J.; Hershey, F. B.; Thorpe, L.; Auer, A. I.; Binnington, B.; Hurley, J. J.; Peterson, G. J.; Schwartz, R.; Woods, J. J., Jr. The use of deep duplex scanning to predict hemodynamically significant aortoiliac stenoses. *J. Vasc. Surg.* 7:395–399; 1988.
- Mo, L. Y.; Yun, L. C. M.; Cobbold, R. S. C. Comparison of four digital maximum frequency estimators for Doppler ultrasound. *Ultrasound Med. Biol.* 14:355–363; 1988.
- Phillips, D. J.; Beach, K. W.; Primozich, J.; Strandness, D. E., Jr. Should results of ultrasound Doppler studies be reported in units of frequency or velocity? *Ultrasound Med. Biol.* 15:205–212; 1989.
- Reddy, D. J.; Vincent, G. S.; MacPharlin, M.; Ernst, C. B. Limitations of the femoral artery pulsatility index with aortoiliac artery: An experimental study. *J. Vasc. Surg.* 4:327–332; 1986.
- Rittgers, S. E.; Thornhill, B. M.; Barnes, R. W. Quantitative analysis of carotid artery Doppler spectral waveforms: Diagnostic value of parameters. *Ultrasound Med. Biol.* 9:255–264; 1983.
- Skidmore, R.; Woodcock, J. P. Physiological interpretation of Doppler-shift waveforms—I. Theoretical considerations. *Ultrasound Med. Biol.* 6:7–10; 1980a.
- Skidmore, R.; Woodcock, J. P. Physiological interpretation of Doppler-shift waveforms—II. Validation of the LaPlace transform method for characterization of the common femoral blood-velocity/time waveform. *Ultrasound Med. Biol.* 6:219–225; 1980b.
- Skidmore, R.; Woodcock, J. P.; Bird, D.; Baird, R. N. Physiological interpretation of Doppler-shift waveforms—III. Clinical results. *Ultrasound Med. Biol.* 6:227–231; 1980c.
- Strandness, D. E., Jr. Echo-Doppler (duplex) ultrasonic scanning. *J. Vasc. Surg.* 2:341–344; 1985.
- Thiele, B. L.; Strandness, D. E., Jr. Accuracy of angiographic quantification of peripheral atherosclerosis. *Prog. Cardiovasc. Dis.* XXVI: 223–236; 1983.
- Tou, J. T.; Gonzales, R. C. *Pattern recognition principles*. Reading: MA: Addison-Wesley Publishing Company; 1974.
- Toussaint, G. T. Bibliography on estimation of misclassification. *IEEE Trans. Info. Theory* IT-20:472–479; 1974.
- Trunk, G. V. A problem of dimensionality: A simple example. *IEEE Trans. PAMI* 1:306–307; 1979.
- Walton, L.; Martin, R. P.; Collins, M. Prospective assessment of the aorto-iliac segment by visual interpretation of frequency analyzed Doppler waveforms—A comparison with arteriography. *Ultrasound Med. Biol.* 10:27–32; 1984.